COMPARATIVE SCALE-RESOLVING AND RANS SIMULATIONS OF A DELTA WING CONFIGURATION

T. Di Fabbio[1], E. Tangermann[1] and M. Klein[1]
[1] Institute of Applied Mathematics and Scientific Computing
Bundeswehr University Munich, Werner-Heisenberg-Weg 39, 85577 Neubiberg, Germany
S. Ketterl[2] and A. Winkler[2]
[2] Division of Flight Physics - Aerodynamics - Aerodynamic Design,
Airbus Defence and Space, 85077 Manching, Germany
tony.difabbio@unibw.de

September 2, 2020

Abstract

The vortex dominated flow around the triple-delta wing aircraft model ADS-NA2-W1 is investigated comparing RANS with scale-resolving DDES results. The Spalart-Allmaras One-Equation Model with corrections for negative turbulent viscosity and Rotation/Curvature (SA-negRC) is employed to close the RANS equations, whereas in the scale-resolving computations the SA-based DDES model is applied. The TAU-Code solver developed by the German Aerospace Center (DLR) is employed in order to perform the numerical simulations. The solutions achieved in the current work are compared with the experimental data provided by Airbus Defence and Space. The aim is a better understanding of the vortex-dominated flows particularly in the transonic speed range in order to determine the range of the suitability of current CFD methods.

Keywords
RANS, Hybrid RANS/LES, SA turbulence model, ADS-NA2-W1 delta wing, vortex formation and breakdown

NOMENCLATURE

AoA, α	Angle of attack	deg
β	Side slip angle	deg
C_L	Lift coefficient	-
C_P	Pressure coefficient	-
d	Distance	m
c_r	Root chord length	m
M	Mach number	-
Re	Reynolds number	-
$S, \tilde{S}$	Strain rate	$1/s$
u, v, w	Velocity components	m/s
ρ	density	Kg/m^3
U_∞	Free stream velocity	m/s
c_∞	Speed of sound	m/s
$t_{characteristic}$	Characteristic time	s
x, y, z	Cartesian coordinates	m
$\Delta_x, \Delta_y, \Delta_z$	Grid spacing	m
Δ	Maximum grid spacing	m
L	Characteristic length	m
μ	Dynamic viscosity	$Kg/(ms)$
ν	Kinematic viscosity	m^2/s
μ_t	Dynamic eddy viscosity	$kg/(ms)$
$\nu_t, \tilde{\nu}$	Kinematic eddy viscosity	m^2/s
P_ν	Production term	-
ϵ_ν	Destruction term	-
ω	Vorticity	$1/s$
$\bar{D}$	Velocity gradient tensor	m/s^2
N_k	Kinematic vorticity number	-
l	Turbulent length scale	m
k	Turbulent kinetic energy	m^2/s^2
ϵ	Turbulent dissipation rate	m^2/s^3
Q	Q-criterion	-

1. INTRODUCTION

Combat aircraft configurations typically feature low aspect ratios and highly swept leading edges in order to provide the required agility. At extreme flight conditions (high angles of attack α and side slip angle β), complex flow fields dominated by vortex systems, which are challenging for numerical flow simulations, are generated. A major challenge in computational fluid dynamics is to model turbulence in order to correctly produce the flow physics at these test conditions.

The investigation of leading-edge vortices of swept wings with low aspect ratio has been subject to research projects within the past decades. Also, unsteady phenomena like the vortex breakdown at high angles of attack have been investigated in detail [6]. Since the flow separation, which forms the initial stage

doi:10.25967/530052

of vortex formation, is fixed by the sharp leading edge, the main challenge of turbulence models is to correctly produce the vortical flow system along the wing surface. With increased complexity of the configuration such as multiple deltas, swept trailing edge, variations of edge contours and other devices of flow control, it is impossible to predict the flow behaviour without detailed simulations.

The numerical simulation of delta wing geometries has been intensively studied for many years due to its complexity and relevance. Reynolds-Averaged Navier-Stokes (RANS) equations and Eddy Viscosity Models (EVM) are considered proper tools for numerical solutions at small to moderate angles of attack. At higher angles of attack, the vortex flow pattern further complicates and the numerical simulations often deviate from experimental data, especially in the vortex regions [5]. The key component of these simulations is the turbulence model and the classical RANS models, which are very efficient in terms of computational time and can be applied for large ranges of computations, are not capable of predicting the flow in these configurations sufficiently accurate. On the other hand, resolving turbulence employing the DNS or LES numerical methods is far too expensive in terms of computational time to apply it on a routine basis. For this reason, only hybrid RANS/LES computations seem to be affordable in order to be performed for selected test cases. Therefore, a model is required, which is capable of predicting flows dominated by leading-edge vortices in a time-efficient and yet accurate manner.

Different methods are present in literature in order to overcome the deficiency of the RANS simulations. Moioli et al. [5] for example aimed to adapt a turbulence model to a specific application of vortex dominated flows. The model terms have been modified in order to achieve better agreement with measured data from experiments.

An interesting research contribution in the field of Hybrid RANS/LES is given by B. Y. Zhou et al. [8]. Hybrid RANS-LES computations have been performed for the turbulent flow around a delta wing at a low subsonic Mach number and the delayed detached eddy simulation with shear-layer adapted (SLA) subgrid scale model in the SU2 open-source solver suite has been applied to predict the vortex breakdown phenomenon. Russell and Schötte [9] have presented the numerical simulation of the flow for the VFE-2 delta wing configuration with rounded leading edges using the Cobalt Navier-Stokes solver. They have achieved reasonable results with both steady RANS and SA-DDES simulations.

The present work aims to provide a contribution in the field of Hybrid RANS/LES numerical methods in order to understand if they are applicable to delta wing simulations at transonic flow condition. In fact, the vortex dominated flow around the triple-delta wing aircraft model ADS-NA2-W1 [2] has been investigated comparing RANS with scale-resolving DDES results and experimental data provided by Airbus D&S. The Spalart-Allmaras One-Equation Model with corrections for negative turbulent viscosity and Rotation/Curvature (SA-negRC) [3] has been employed to close the RANS equations, whereas in the scale-resolving computations the SA-based DDES model has been applied [1]. The current study aims to analyze the capability of Hybrid RANS/LES method in order to predict the flow behaviour around a delta wing at these flight conditions. DLR TAU-Code and SuperMuc-NG resources have been employed in order to perform the simulations.

2. Turbulence Model and Numerical Methods

The complex turbulence fluctuations in the flow field are captured by the underlying turbulence models. Generally, these turbulent fluctuations are represented by the Reynolds-stress tensor in the momentum equation. Different assumptions are used for modeling the Reynolds-stress tensor, which categorizes the type of the turbulence model used in the solver. The widely used Boussinesq assumption relates the stress tensor linearly to the velocity gradients by means of the turbulent viscosity.

In the case of the one-equation eddy viscosity turbulence model (SA-model), one transport equation is used to describe the transport of one scalar (the turbulent viscosity). Due to the simplification for the Reynolds-stress tensor, the turbulence model is not well suited for flows where stress and strain rates are not aligned or where a rapid redistribution among the stresses takes place. A primary deficiency with the eddy viscosity models appears in their inability to account for turbulent anisotropies in rotating and separated flows. In order to fix this issue and correct the SA turbulence model, vortical correction methods have been implemented.

All simulations have been performed using the DLR TAU-Code release.2019.1.0 flow solver developed by the German Aerospace Center [4]. The TAU-Code is a 2nd order finite volume flow solver, fully parallelized, for unstructured hybrid grids. It is useful to run a RANS simulation first and then use the results to choose a criterion for the hybrid RANS/LES mesh because these methods require a time-accurate simulation and a fine 3-D grid. Instead of modeling the entire turbulent spectrum, it is possible to resolve parts

of the spectrum by means of a scale-resolving simulation, using either Large-Eddy simulation (LES) or hybrid RANS/LES. Delayed-detached-eddy simulation (DDES) provides a single non-zonal formulation for using a RANS model in boundary layers and to switch to LES mode in regions of massive separation.

2.1. Hybrid RANS/LES method

In the present work the Spalart-Allmaras model that represents a standard RANS closure for aerodynamic applications is employed for the Hybrid RANS/LES simulations as well.
The SA-DDES model [13] is based on the one-equation model by Spalart-Allmaras model [12] for the eddy viscosity

$$(1)\quad \frac{\partial}{\partial t}(\rho\tilde{\nu}) + \vec{u}\cdot\vec{\nabla}(\rho\tilde{\nu}) = \\ + \vec{\nabla}\cdot\left(\frac{\mu+\rho\tilde{\nu}}{\sigma}\vec{\nabla}\tilde{\nu}\right) + \rho\frac{c_{b2}}{\sigma}(\vec{\nabla}\tilde{\nu})^2 + P_\nu - \epsilon_\nu,$$

where the production term P_ν and the destruction term ϵ_ν are respectively

$$(2)\quad P_\nu = c_{b1}\rho\tilde{S}\tilde{\nu} \qquad and \qquad \epsilon_\nu = c_{w1}f_w\rho\left(\frac{\tilde{\nu}}{\tilde{d}}\right)^2.$$

This is exactly the original SA-model, except that the length scale d resp. $\tilde{d}$ in the destruction term is modified. In the SA-model, d is the distance to the nearest wall [11]. In the DDES model, d is replaced with $\tilde{d}$, which is defined as

$$\tilde{d} = min(d, C_{DES}\Delta)$$

with $\Delta = max(\Delta x, \Delta y, \Delta z)$, where $\Delta x, \Delta y, \Delta z$ denote the grid spacing in x-, y-, and z-direction resp.
Defining $\Delta = max(\Delta x, \Delta y, \Delta z)$ ensures RANS behavior in boundary layers as $d \ll \Delta$, although $\Delta y \ll d$ and the ratio between $(\Delta x\Delta y\Delta z)^{1/3}$ and d is unclear.
Moreover, the low-Re modification of the DES length-scale by Strelets is implemented

$$\tilde{d} = min(d, \Psi C_{DES}\Delta)$$

with

$$\Psi^2 = \frac{1 - c_{b1}f_{v2}/(c_{w1}K^2f_w^*)}{f_{v1}}$$

and $f_w^* = 0,427$ [15].

2.1.1 DDES numerical approach

Taking the Hybrid RANS/LES simulations into account, in order to stabilize the solver, unsteady simulations are performed with an implicit dual-time stepping approach, employing a Backward-Euler/LUSGS implicit smoother. The chosen time step has to adequately resolve the time scales of the energy containing eddies in the flow of interest [7]. To ensure convergence of the inner iterations, it is recommended to use the Cauchy convergence criterion in combination with useful metrics. Integral quantities such as lift and drag provide an indirect measure of the convergence of second-order quantities.
A suitable CFL (Courant-Friedrichs-Lewy) number is set in order to obtain stable convergence of the solution. The computation of the fluxes have been performed with a central scheme and the matrix dissipation model has been selected [15]. However, in LES and hybrid RANS/LES the artificial dissipation should be reduced in order to prevent excessive damping of the resolved turbulent structures [14].
Moreover, it is useful to run a RANS simulation first and then use the results to choose the criterion for the DES/LES mesh. In fact, the turbulence length scale in Eq. 3 is a physical quantity describing the size of the large energy-containing eddies in a turbulent flow and has to be bigger than the cells size. In other words, the cell size shall be small enough to capture the turbulent behaviour and fluctuations in the LES region. The turbulence length scale is expressed as follows

$$(3)\quad \Delta < l = C_\mu\frac{k^{\frac{3}{2}}}{\epsilon},$$

where C_μ is an empirical constant specified in the turbulence model (approximately 0.09), k the turbulent kinetic energy and ϵ the turbulent dissipation rate.

2.2. RANS Turbulence Model

The Negative Spalart-Allmaras One-Equation Model (SA-neg) with corrections for Rotation/Curvature (SA-negRC) is employed to close the RANS equations. The SA-neg model is the same as the "standard" version (SA) when the turbulence variable $\tilde{\nu}$ is greater than or equal to zero. The Eq. 1 is modified and the turbulent eddy viscosity (μ_t) in the momentum and energy equations is set to zero when the kinematic eddy viscosity becomes negative [11].
The SA turbulence model often provides excessive eddy viscosity production in the vortex, with implications on the unburst vortex size, type and velocities. Experience has shown that the main source of error is usually due to a wrong prediction of the eddy viscosity destruction in the vortex flow regions due to the limitation of standard RANS models to accurately represent highly rotational regions. Shur et al. [10] proposed a streamline curvature correction (SA-RC) which alters the source term with a correction function multiplying the production term of the eddy viscosity

transport equation. The SA-RC correction for Rotation and Curvature is sometimes able to improve the quality of the simulations but there are also scenarios where the prediction quality deteriorates.
The production term (2) of the eddy viscosity transport equation is multiplied by a "rotation function" written as follows

(4) $$f_{rotation} = (1 + c_{r1}) \frac{2r^*}{1 + r^*} \left[1 - c_{r3} tan^{-1}(c_{r2}\tilde{r})\right] - c_{r1}$$

with the constants c_{r1}, c_{r2} and c_{r3} calibrated as 1, 12 and 1 respectively [11].
A vortex identifier quantity is required to be coupled with the additional terms in order to exclusively influence the vortex region and the SA-RC modification suggests the possibility to use the ratio between the strain rate S and vorticity ω

$$r^* = \frac{S}{\omega} = \frac{1}{N_k}$$

The definition is correlated to the kinematic vorticity number N_k, defined by Truesdell [10].

2.2.1 RANS numerical approach

The steady RANS simulations have been performed using a multigrid relaxation employing a Backward-Euler/LUSGS implicit smoother. An AUSMDV upwind scheme is used for the flux discretisation; it is an improved Advection Upstream Splitting Method (AUSM) which combines the flux Difference (AUSMD) and the Vector splitting (AUSMV) methods [14]. The CFL number is reduced starting from a large value in order to find the best compromise between speed and stability. The entire model is simulated in a fully turbulent flow. All computations are conducted using the SA-neg turbulence model with the SA-RC correction (abbreviated as SA-negRC).

3. Results and Discussion

3.1. ADS-NA2-W1 Test Case

The ADS-NA2-W1 model illustrated in Fig. 1, available within this study, features a sharp leading edge [2]. The transonic regime of $M = 0,85$ and $Re = 12,53 \cdot 10^6$ has been selected for the simulations. The experimental data for this model are provided by Airbus Defence and Space.
The definition of the Characteristic Time is given as follows

(5) $$t_{characteristic} = L/U_\infty$$

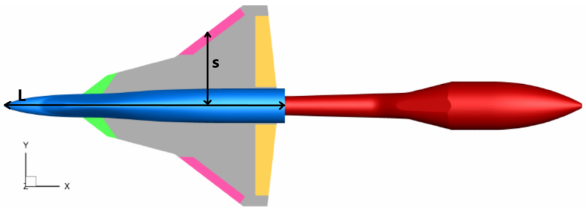

Figure 1: NA2 model configuration

where L is the length of the model (characteristic length) and U_∞ the free stream velocity. It is the time that a fluid flow volume takes to pass through the model and it is important to take this definition during an Hybrid RANS/LES simulations with the dual-time stepping scheme into account in order to understand how much physical or computational time is necessary to obtain a reliable solution. Ten flow trough times are taken into account in order to compute the mean values of the flow proprieties. The Characteristic Time expressed in Eq. 5 for the ADS-NA2-W1 model is computed as follows

$$M = 0,85 \rightarrow U_\infty = c_\infty \cdot M \approx 280,41\ m/s$$

where $c_\infty \approx 330\ m/s$. Consequently,

$$t_{characteristic} \approx 2 \cdot 10^{-3}\ s$$

The computational domain employed to investigate the ADS-NA2 model [2] consists of about *40 millions elements*. In order to capture "correctly" the flow characteristics, the convective CFL number has to be lower than 1 in each cell of the mesh. The time step size in the dual-time ("unsteady time stepping" in DLR TAU-code) is set equal to $5 \cdot 10^{-7}\ s$ with the aim of satisfying the previous requirement.

3.2. Analysis of different methods

Different simulations have been performed with constant side slip angle $\beta = 5°$, that emphasizes the asymmetry of the turbulent flow, varying the angle of attack between $12° < \alpha < 28°$. The transonic regime of $M = 0.85$ and $Re = 12.53 \cdot 10^6$ has been selected. Fig. 2 and 3 shows the lift coefficient curve and the rolling moment coefficient curve, respectively. The experimental data provided by Airbus D&S are plotted in comparison with the RANS and the DDES results. DDES have been performed only for $\alpha = 12°, 24°$.
The RANS and DDES results overestimate the experimental lift data but it is worth noting that the DDES are closer to the experimental ones. Fig. 3 shows a smooth transition between the RANS and DDES points but what happens in between is not known and documented in literature. Although the sharp drop of the curve for $AOA = 24°$ has not been predicted, it

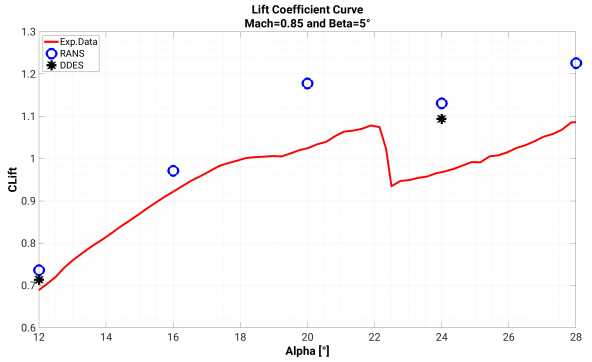

Figure 2: Lift Coefficient over AoA

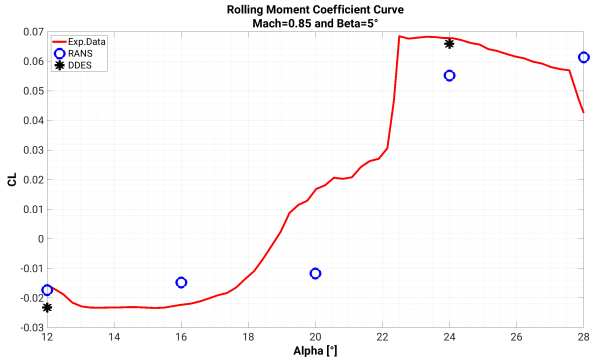

Figure 3: Rolling Moment Coefficient over AoA

is remarked that this is the first step and further improvements will be investigated employing the Hybrid RANS/LES method. In particular, it could be interesting to analyze what happens if the AoA steps become smaller, for example, a drop or a smooth decay of the lift curve could be achieved. The DDES method appears to be a promising tool to simulate the flow physics around a delta wing at transonic condition. This is confirmed also by the roll moment plotted in Fig. 3 that is particularly interesting with slide slip. In fact, the roll moment also reacts "more sensitively" than the coefficient of lift when the flow pattern is more accurate due to the different simulations setup.
The flow pattern of the ADS-NA2-W1 test case is further complicated by the presence of vortex merging caused by the presence of multiple sweep angles as illustrated in Fig. 1. The side slip angle of $\beta = 5°$ amplifies the asymmetry of the flow and generates two different flow conditions over the two sides of the wing. In order to visualize all these phenomena in more detail the simulation results at $\alpha = 24°$ are considered.
Fig. 4 shows the comparison of the surface coefficient of pressure on the model by matching experimental data, RANS SA-negRC and SA-DDES results. Moreover, as it can be seen in Fig. 4a six different slice planes are taken into account. The

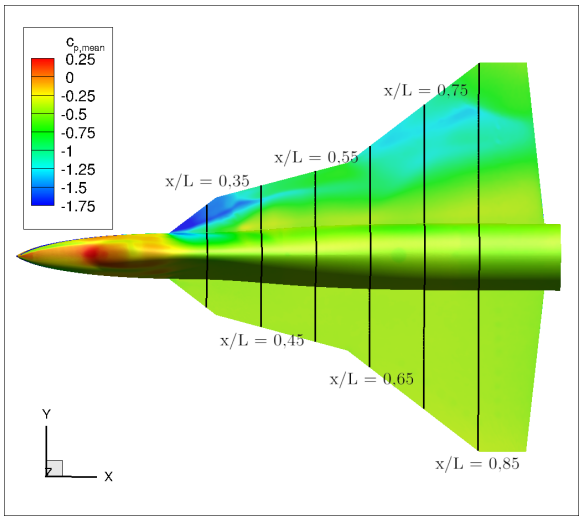

(a) Experimental Data

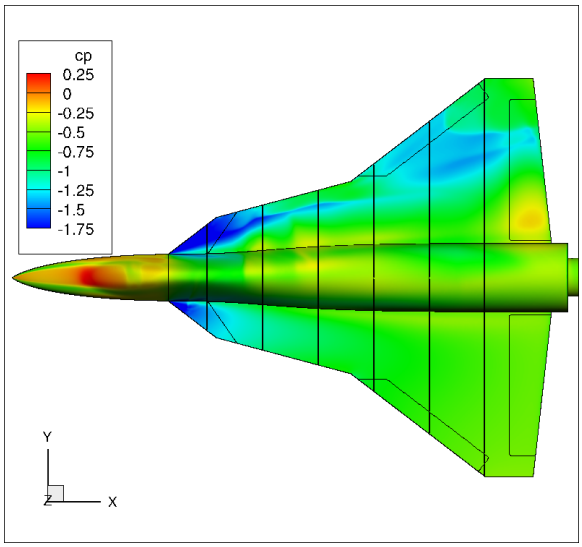

(b) RANS

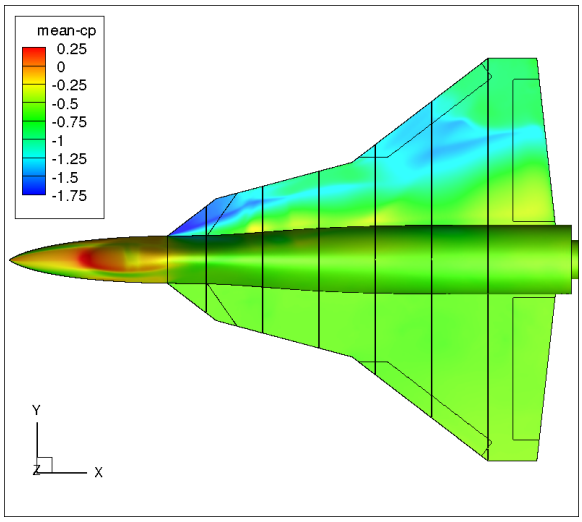

(c) DDES

Figure 4: Surface coefficient of pressure, comparison between experimental data, RANS SA-negRC and SA-DDES results for the ADS-NA2-W1 model with $M = 0.85$, $Re = 12.53 \cdot 10^6$, $\alpha = 24°$ and $\beta = 5°$

surface coefficient of pressure distribution along the spanwise direction at chordwise positions $x/c_r = 0.35,\ 0.45,\ 0.55,\ 0.65,\ 0.75,\ 0.85$[1] is plotted in Fig. 6. Moreover, Fig. 7 shows the axial velocity u distribution at chordwise locations $x/c_r = 0.35,\ 0.55,\ 0.75$, by doing a comparison between RANS SA-negRC and SA-DDES results, in the left and right column, respectively. [2]

At these transonic flow conditions a vortex breakdown appears and the SA-models fail to predict the correct flow physics. This occurs in particular for the RANS simulations but it is not possible to exclude the same issue employing the SA-DDES model after the present work.

As illustrated with the iso-surface ($Q = 1 \cdot 10^7$) in Fig. 5, the flow is not attached around the leading edge and separates in a vortex sheet. In particular, two different vortices are present on the starboard wing and the breakdown on the portside wing[3].

Q is one invariant of the velocity gradient tensor. Using the decomposition into symmetric and anti-symmetric parts this invariant can be expressed as follows.

$$Q = \frac{1}{2}\left(tr(\bar{D})^2 - tr(\bar{D^2})\right) = \frac{1}{2}|\bar{\omega}|^2 - |\bar{S}|^2 \tag{6}$$

Q represents the local balance between shear strain rate and vorticity magnitude, defining vortices as areas where the vorticity magnitude is greater than the magnitude of rate-of-strain.

Fig. 5 shows that the separation onset occurs in correspondence with the two wing apexes. The two generated fully developed vortices interact with each other in the rear part of the starboard wing. The angle of attack directly influences the vortex behaviour and due to its value, no vortex breakdown phenomenon is evident on the starboard wing. For this reason, it is still possible to distinguish the two different vortices in Fig. 7 at the chordwise location $x/c_r = 0,75$ where the two peaks of axial velocity are located. In particular, the DDES results (on the right side in Fig. 7) show that the vortex are merging and interacting with each other.

Fig. 4a shows the experimental surface coefficient of pressure on the upper side of the aircraft. The suction footprint on the wing surface is caused by the high tangential velocity around the inner vortex core. In fact, in the case of low aspect ratio delta wings, the generated vortex sheet is highly influenced by the pressure gradients in its vicinity and its separation at the swept leading edge causes a local low pressure region on the suction side which contributes to the overall lift. However, the so-called vortex lift has a

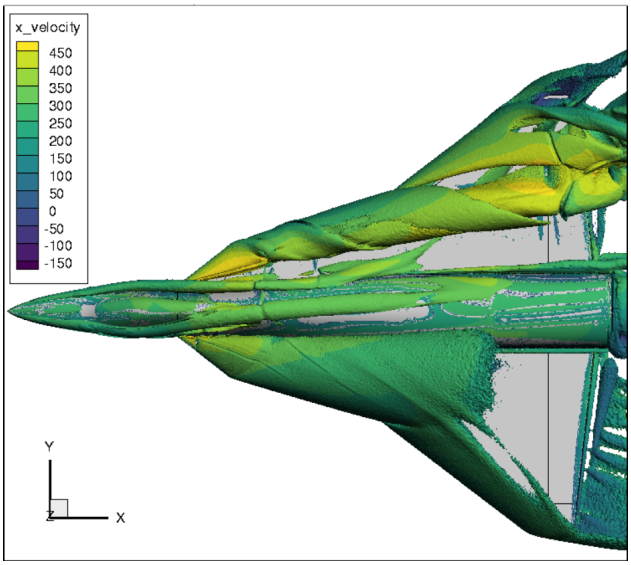

(a) RANS

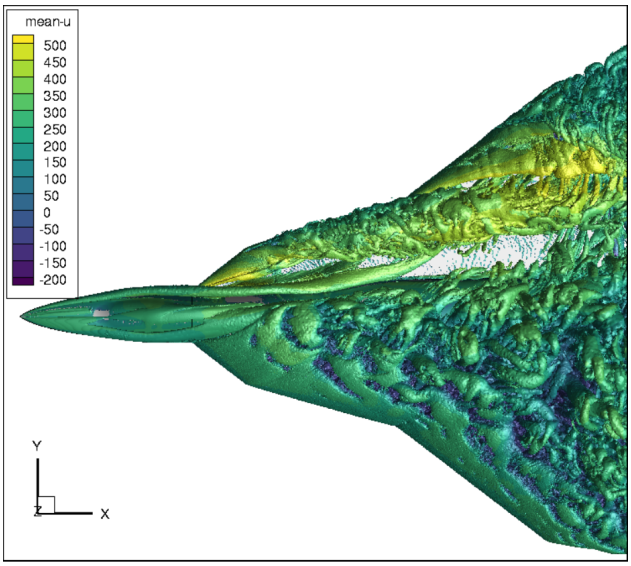

(b) DDES

Figure 5: Q-criterion iso-surface drawn at $Q = 1 \cdot 10^7$ with flood contour by x-velocity u, comparison between RANS SA-negRC and SA-DDES results for the ADS-NA2-W1 model with $M = 0.85$, $Re = 12.53 \cdot 10^6$, $\alpha = 24°$ and $\beta = 5°$

[1] Here, $c_r = L$ in order to simplify the further considerations.

[2] Regarding the DDES results, the mean values of the flow proprieties computing over 10 flow trough times are taken into account.

[3] The nautical labeling: starboard ($y > 0$) and port(side) $y < 0$

limiting AoA at which the vortex bursts or breaks down. In other words, the use of vortex lift is restricted by vortex breakdown or bursting and an inherent instability. This consists of an abrupt change in the flow topology where the flow decelerates and diverges as if a solid obstacle was present in the flow. The structure of the vortex varies slowly in the streamwise direction and then, suddenly, the structure changes drastically with the formation of an axisymmetric recirculation region. In fact, whereas vortices will diffuse in the flow field under normal conditions, vortex breakdown is encountered in some special cases. The location and mode of breakdown depends on various parameters such as adverse pressure gradients, type of delta wing planforms, angle of attack, sweep angle. For these reasons, the vortex generation at the swept leading edge dominates the aerodynamic characteristics of the wing and its understanding and prediction are of primary importance.

The unburst part of the vortex present on the starboard side of the model is characterized by a coherent structure with high values of axial velocity, as it can be seen also in Fig. 7, and rotational velocity in which the vorticity increases along the axial direction. Downstream the breakdown present on the portside of the wing, the flow becomes incoherent and turbulent, as the hybrid RANS/LES results in Fig. 5b shows. Moreover, Fig. 7 demonstrates that the vortex breakdown is always accompanied by an expansion of the vortex core and an abrupt reduction of axial and rotational velocities. Consequently, the suction footprint on the wing surface is significantly reduced on this part of the wing (see Fig. 6).

In this selected test case, over the starboard part of the wing, the flow undergoes a primary separation at the wing leading edge and subsequently rolls up to form a stable, separation-induced leading-edge vortex. An illustration of this vortex behavior is shown in Fig. 5a and 5b. The primary vortex induces reattached flow over the wing, and the spanwise flow under the primary vortex subsequently separates a second time to form a counter-rotating secondary vortex outboard of the primary vortex[4]. This phenomenon is visible in Fig. 6 at the chordwise station $x/c_r = 0,45$ close to the "positive" leading edge ($y/s = 1$) and in Fig. 7 at the chordwise location $x/c_r = 0,55$. The DDES simulations capture the secondary vortex formation but they overestimate the coefficient of pressure in that region. The flow under the vortices induces significant upper surface suction pressure that results in large vortex-induced lift increments.

Fig. 6 shows the surface coefficient of pressure distribution over the wing and the SA-negRC RANS simulations mispredict the flow pattern over the portside part of the wing in particular closer to the wing apex due to high turbulence and chaotic behaviour of the flow. On the contrary, DDES seems to be able to capture the right flow physics even if they overestimate the intensity of the suction footprint.

Taking the starboard side of the wing into account, the side against which the wind predominantly comes, the results need more attention. In the first part of the wing, $x/c_r < 0,55$ it is evident how the DDES improves the results of the simulations. Fig. 7 at the chordwise location $x/c_r = 0,35$ shows that only the DDES simulation is able to capture the separation and the reversed flow over the front part of the starboard wing. Moreover, it will be useful to visualize the slice plane at the chordwise location $x/c_r = 0,55$ in Fig. 4a placed before the second increment of the delta angle on the wing. Afterwards, the second vortex is generated, it merges with the first one and the DDES results became less reliable, as it can be seen in Fig. 6. This phenomenon can explain the overestimation of the lift coefficient in Fig. 3 and will be investigated in more detail in future work.

It is possible to note from Fig. 6 that the trend of the DDES results of the surface C_p distribution along the spanwise direction at different chordwise station is always similar to the experimental data for $x/c_r < 0,85$. This demonstrates that the correct flow pattern is captured by the DDES method even if the suction footprint over the model is overestimated.

All these considerations demonstrate that interesting and promising improvements have been achieved employing the SA-DDES numerical method. The results of the DDES on the portside side are positive. The vortex is too stable on the starboard side. This could be due to the mesh resolution inside the vortex core or it could indicate that a pure SA model without vortex correction is also not sufficient for DDES. The discrepancies between SA-DDES results and experimental data are in particular evident only in the rear part of the starboard wing where the two generated fully developed vortices merge and interact with each other. Slight quantitative deviations have been highlighted but the illustrated qualitatively results clearly show that all the hours spent on DDES have been worth. In fact, the DDES shows most of the important flow features which are missing in the RANS, as for example the vortex breakdown flow characteristics, the secondary vortex formation and the interaction between the first and second vortex.

[4]The secondary vortex is the counter-rotating one, whereas the second vortex is the outer one resulting from the different sweep angles.

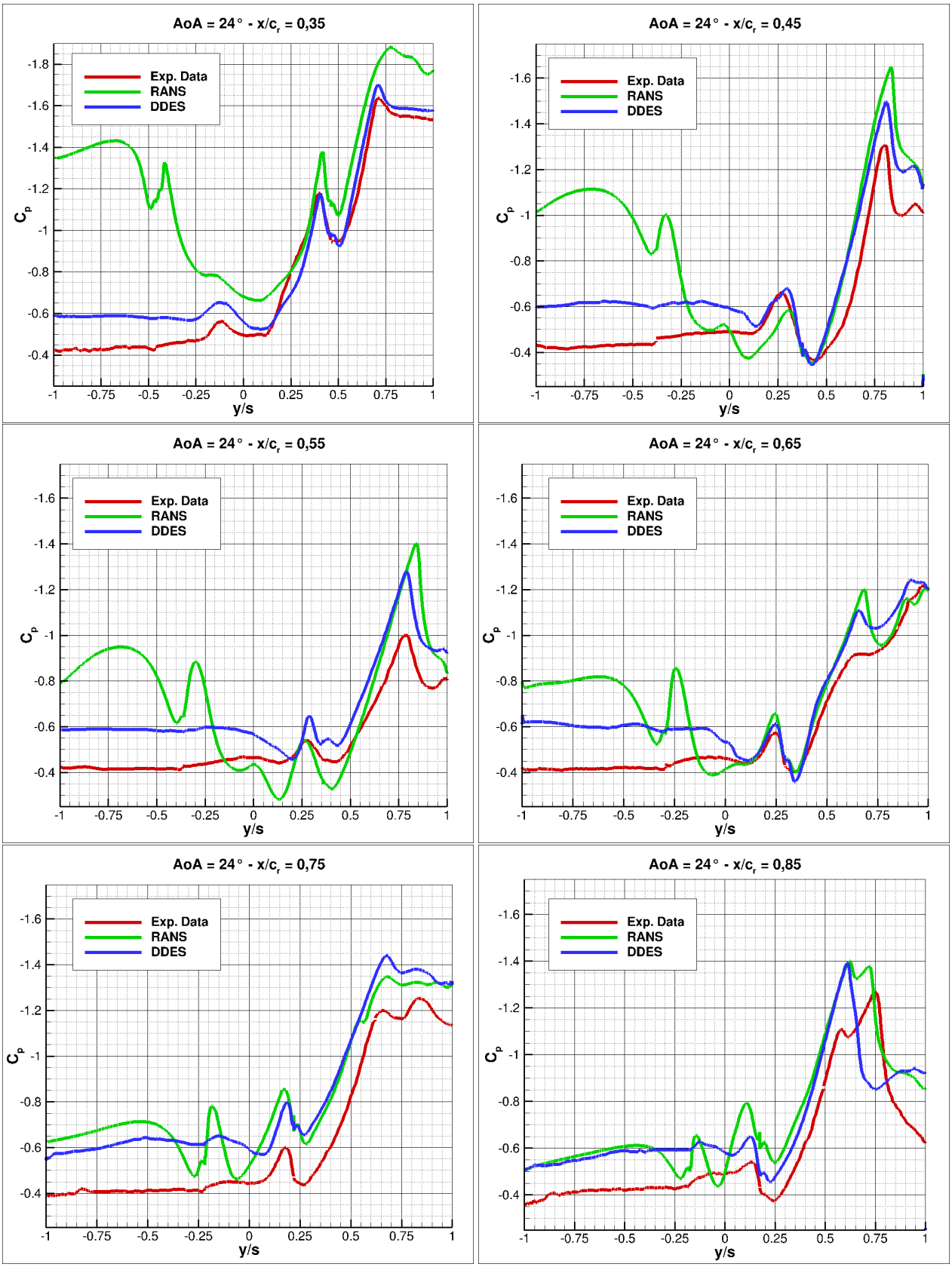

Figure 6: Surface C_p distribution, comparison between experimental data, RANS SA-negRC and SA-DDES for the ADS-NA2-W1 model with $M = 0.85$, $Re = 12.53 \cdot 10^6$, $\alpha = 24°$ and $\beta = 5°$

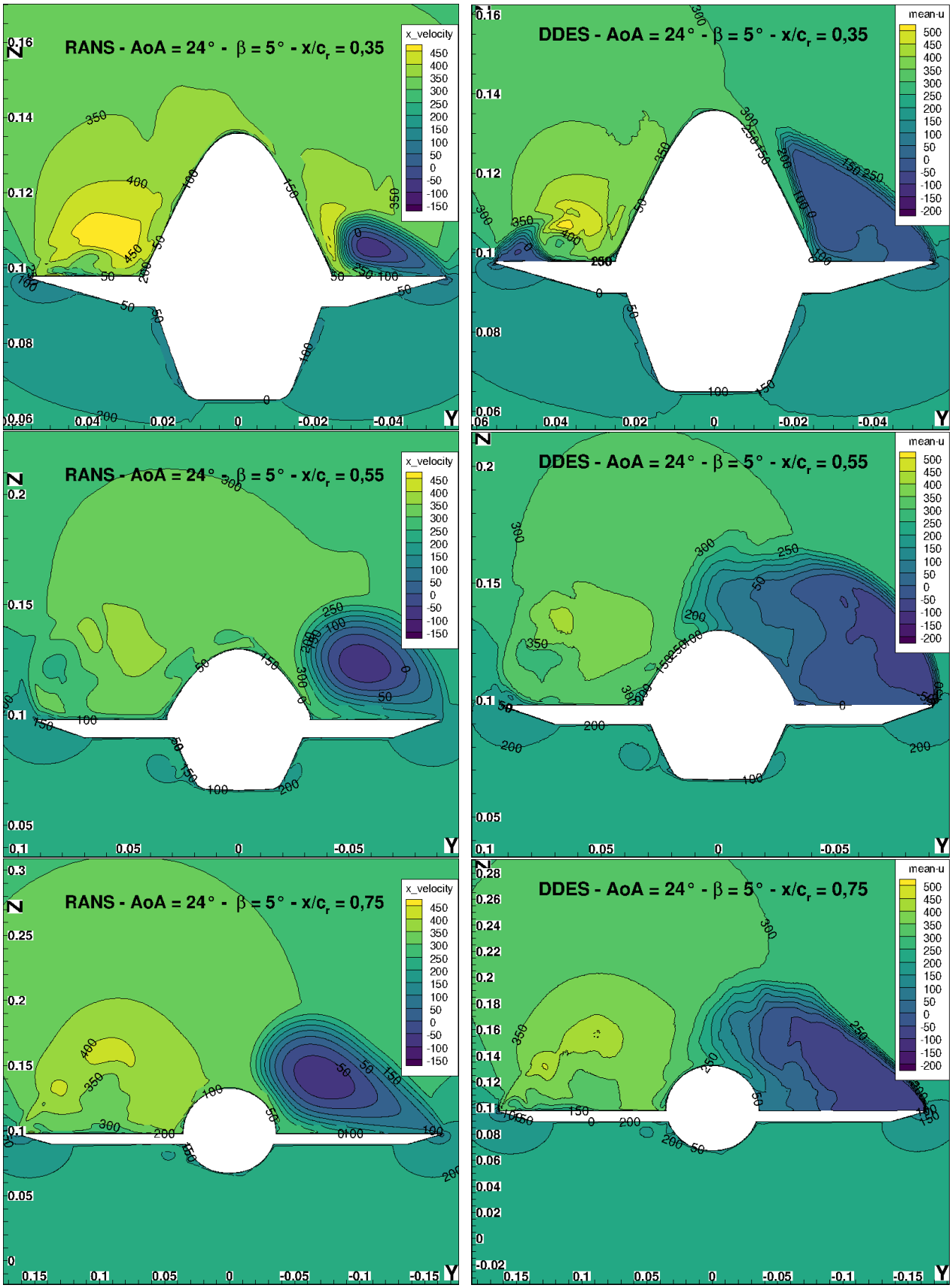

Figure 7: Axial velocity u contour plots at chordwise locations $x/c_r = 0.35,\ 0.55,\ 0.75$, comparison between RANS SA-negRC (on the left column) and SA-DDES (on the right side) results for the ADS-NA2-W1 model with $M = 0.85$, $Re = 12.53 \cdot 10^6$, $\alpha = 24°$ and $\beta = 5°$

4. Conclusions and Outlooks

The vortex dominated flow around the triple-delta wing aircraft model ADS-NA2-W1 has been investigated comparing RANS with scale-resolving DDES results and experimental data provided by Airbus D&S. The Spalart-Allmaras One-Equation Model with corrections for negative turbulent viscosity and Rotation/Curvature (SA-negRC) has been employed to close the RANS equations, whereas in the scale-resolving computations the SA-based DDES model is applied. The transonic regime of $M = 0,85$ and $Re = 12,53 \cdot 10^6$ has been selected and the ADS-NA2-W1 model with the sharp leading edge profile generates flow separation along the entire leading-edge at selected $AoA = 24°$. Based on the pressure gradients over the suction side, occurrences of secondary vortex have been observed taking the DDES results in particular into account.
However, even if a sharp leading-edge geometry implies that the separation takes place over the whole leading-edge extension, the solution of the vortex flow lacks accuracy. The RANS turbulence model provides excessive eddy viscosity production in the vortex, with implications on the unburst vortex size, type and velocities. Consequently, the suction peak and the pressure distribution differ from experiments. The secondary vortex is stronger, shifted and hence affecting also the main vortex position and development. The breakdown is misrepresented by RANS numerical solutions and, consequently, the surrounding flow and the post-breakdown region are also negatively affected.
Interesting and promising improvements have been achieved employing the SA-DDES numerical method. Good results are obtained in the front part of the wing where only the first vortex is developed. The discrepancies between SA-DDES results and experimental data are evident in the rear part of the starboard wing where the two generated fully developed vortices merge and interact with each other. In particular, the qualitatively results illustrated in Section 3 clearly show that all the hours spent on DDES have been worth. The DDES shows most of the important flow features which are missing in the RANS and this is exactly the purpose of the present paper.
Since it appears that the model is reliable in the presence of one single vortex, the fine-tuning of the method will be carried out and the investigation of vortex merging and interaction is strictly recommended.
Moreover, taking regions of attached and separated flow into account, shielding function in the DES method is expected to further improve the results in future work.

Acknowledgments

The funding of this investigation by Airbus Defence and Space within the project "Efficient Turbulence Modelling for Vortical Flows from Swept Leading Edges" is gratefully acknowledged as well as the support with experimental data of the ADS-NAS-W1 model. The authors gratefully acknowledge the German Aerospace Center (DLR) for providing the DLR TAU-Code used for the numerical investigation of the present research. Moreover, the authors thank to the Gauss Centre for Supercomputing for funding this project by providing computing time on the GCS Supercomputer SuperMUC at Leibniz Supercomputing Center (account number pn68zu).

References

[1] S. R. Allmaras, F. T. Johnson and P. R Spalart, *Modifications and Clarifications for the Implementation of the Spalart-Allmaras Turbulence Model*, ICCFD7-1902, 7th International Conference on Computational Fluid Dynamics, Big Island, Hawaii, 2012.

[2] A. Hovelmann, A. Winkler, S.M. Hitzel , K. Richter and M. Werner , *Analysis of Vortex Flow Phenomena on Generic Delta Wing Planforms at Transonic Speeds*, New Results in Numerical and Experimental Fluid Mechanics XII, Contributions to the 21st STAB/DGLR Symposium, Darmstadt, Germany, 307-316, 2018.

[3] P. R. Spalart, S. Deck, M. L. Shur , K.D. Squires, M. K. Strelets and A. Travin, *A new version of detached-eddy simulation resistant to ambiguous grid densities*, Theoretical and Computational Fluid Dynamics, Vol. 20, Pag. 181-195, 2006.

[4] S. Langer, A. Schwöppe and N. Kroll, *The DLR Flow Solver TAU - Status and Recent Algorithmic Developments*, 52nd Aerospace Sciences Meeting, National Harbor, Maryland, USA, 2014.

[5] M. Moioli, C. Breitsamter and K. A. Sorensen, *Turbulence Model Conditioning for Vortex Dominated Flows Based on Experimental Results*, ICAS [31st, Belo Horizonte, 2018], 2018.

[6] A. Elsenaar, L. Hjelmberg, K. Butefisch and W. J. Bannik, *The International Vortex Flow Experiment*, AGARD Fluid Dynamics Panel Symposium on Validation of Computational Fluid Dynamics, No. 437, Vol. 1, 1988.

[7] P.R. Spalart, *Young person's guide to detached-eddy simulation grids*, Technical report, NASA-2001-cr211032, 2001.

[8] B. Y. Zhou, N. R. Gauger et al., *Hybrid RANS/LES Simulation of Vortex Breakdown Over a Delta Wing*, Computational Fluid Dynamics Conference at AVIATION Forum, 17 - 21 June 2019, Dallas, USA.

[9] R. M. Cummings and A. Schütte, *Detached-Eddy Simulation of the vortical flow field about the VFE-2 delta wing*, Aerospace Science and Technology, 24(1), Pag. 66-76, 2012.

[10] M. L. Shur et al., *Turbulence Modeling in Rotating and Curved Channels:Assessing the Spalart-Shur Correction*, AIAA JOURNAL, Vol. 38, No. 5, May 2000.

[11] C. Rumsey, *Turbulence Modeling Resource*, Langley Research Center, https://turbmodels.larc.nasa.gov/spalart.html, 2020.

[12] P. R. Spalart and S. R. Allmaras, *A One-Equation Turbulence Model for Aerodynamic Flows*, AIAA-92-0439, 1992.

[13] P. R. Spalart, W. H. Jou, M. Strelets, S. R. Allmaras, *Comments on the feasibility of LES for wings, and on a hybrid RANS/LES approach*, First AFOSR International Conference on DNS/LES, Ruston, LA, 4-8, August, 1997, in: Advances in DNS/LES, edited by C. Liu and Z. Liu (Greyden, Columbus, OH, 1997).

[14] *TAU-Code User Guide release 2019.1.0*, DLR Institute of Aerodynamics and Flow Technology.

[15] *Technical Documentation of the DLR TAU-Code release 2019.1.0*, DLR Institute of Aerodynamics and Flow Technology.

[16] M. Moioli, C. Breitsamter and K. Sørensen, *Turbulence Modeling for Leading-Edge Vortices: an Enhancement based on Experimental Data*, IAA SciTech Forum, 10 January 2020, Orlando, FL